Materials Advances

ROYAL SOCIETY OF CHEMISTRY

PAPER

View Article Online
View Journal | View Issue

Cite this: *Mater. Adv.*, 2022, 3, 5521

Keggin based self-assembled mesoporous materials for the capture of selective guest molecules†

Kesar Tandekar, Anjali Tripathi, Muvva D. Prasad ‡ and Sabbani Supriya *

A series of self-assembled mesoporous materials, compounds **1–9**, of the type $[RPPh_3]_n[XM_{12}O_{40}]$ (R = Ph, Me, Et; n = 3 or 4; X = P, Si; M = Mo, W) composed of Keggin anions and phosphonium cations have been fabricated and characterized. These thermally stable hybrid materials show selective reversible uptake of non-polar molecules such as iodine and carbon disulfide under ambient conditions. The resultant porosity is attributed to the self-assembling of the cations on the surface of the Keggin anion such that the pores are lined with the phosphonium cations rendering them hydrophobic. The present work explores the spontaneous self-assembly process of POM integrated mesoporous compounds stabilized *via* non-covalent interactions and their potential applications as adsorbing materials.

Received 18th November 2021,
Accepted 16th May 2022

DOI: 10.1039/d1ma01092a

rsc.li/materials-advances

Introduction

Efforts to achieve/promote spatial organization *via* self-assembly of small building blocks have been made constantly.[1] Among the huge plethora of building units available, construction of ordered nanomaterials integrated with polyoxometalates (POMs) as molecular building blocks are particularly sought after primarily due to the resultant properties and applications. The construction of the nanostructured assemblies, obtained by the functionalization of POM clusters with organic units in an ion exchange reaction, is an ingenious technique for the formulation of new functional materials.[2–6] This strategy provides for the combination of the properties of both the POMs and the organic units in a synergistic manner. In such systems, the anionic POM and the organic moieties which act as the cations are held together by non-covalent interactions.[7–10] Among the prevalent non-covalent interactions of the type van der Waals forces, hydrogen bonding and π–π stacking, complexes stabilized by electrostatic interactions are particularly desirable.[11–13] Even though, nano-sized POMs have been exploited extensively for their catalytic and adsorption properties, their low solubility in organic solvents and high crystalline energy hamper their applications in many fields.[14,15] The organic–inorganic hybrid POM materials, hence, are highly lucrative as they are more accessible by the organic as well as the biological media which further their application spectrum to capturing bulky molecules, drug delivery and as heterogeneous catalysts. Self-assembly is one of the routes through which the materials aspects of POMs can be honed. The simple process of self-assembly can result in the formation of smart responsive systems,[16–19] liquid crystals,[20–25] micellar and micro-emulsion systems,[26–31] hollow spheres/vesicles[5,32–35] and porous materials.[36–39] Designing porous materials out of POMs is extremely attractive. POM-based porous materials can be generated by the combination of POMs with different metal–organic frameworks (MOFs), coordination polymers (CPs), organic amines and surfactants as well as by immobilization on porous silica and carbon substrates.[46] POMs which display uniform particle size, specific surface charges and well-defined topologies exhibit augmented surface areas when designed into hybrid porous materials. Amalgamation of the inherent characteristics of POMs with their newly acquired properties enables the usage of porous POM-hybrid materials in a multitude of applications such as gas adsorption, hydrogen storage, catalysis, super-capacitors and hydrogen evolution.[40–52]

Much attention has been devoted to porous materials because of the possible interactions between their pore walls and incoming atoms, ions or molecules. Their versatility is further enhanced by the ability to control their pore sizes during synthesis which in turn facilitates the uptake of several gaseous, liquid and solid guests. Additionally, they have been understood to be substances of scientific and technological importance.[53,54] The synthetic routes to porous materials[55–61] primarily involve the templating strategies apart from the many other techniques which require extensive work-up and can be

School of Physical Sciences, Jawaharlal Nehru University, New Delhi 110067, India. E-mail: ssabbani@jnu.ac.in, sabbani07@gmail.com

† Electronic supplementary information (ESI) available. See DOI: https://doi.org/10.1039/d1ma01092a

‡ Present address: Central Sophisticated Instruments Facility (CSIF), Birla Institute of Technology and Science Pilani, K K Birla Goa Campus, South Goa-403726, India.

tedious. In such a scenario, porous hybrid materials generated during a facile, spontaneous self-assembly process in the absence of any external template, is highly remarkable. Depending on their pore shape and size, and counter cations, these porous materials can be utilized for selective trapping of molecules as well as catalysts (both homogeneous and heterogeneous) to drive certain dormant reactions in aqueous, organic as well as biphasic media. As such, there are many reports related to the synthesis of POM-based porous materials using a variety of techniques[48–52] but those obtained *via* self-assembly process are rare. One of the important contributions is reported by Wei, Zhang and their co-worker in which they have demonstrated reversible iodine capture by polyoxometalate based 2D nanostructures.[62]

Herein we report a series of solid, polycrystalline POM associated mesoporous hybrid materials **1–9** of the type $[RPPh_3]_n[XM_{12}O_{40}]$ (where R = Me, Et, Ph; X = Si, P; M = Mo, W; n = 3 or 4). These materials are formed due to the spontaneous aqueous phase self-assembly reaction of POM anion and organic phosphonium cations, forming spherical aggregates, the two moeities being held together by electrostatic interactions. Interestingly, the porosity of these complexes is due to the self-assembly of the spherical aggregates composed of Keggin anions and phosphonium cations. The adsorption properties of these porous materials have further been studied. The mesoporous structure of the synthesized POM hybrid materials and the hydrophobic nature of their pores enable the successful reversible uptake of selective guests such as iodine (I_2) and carbon disulfide (CS_2) under ambient conditions.

Experimental section

All the chemicals (phosphomolybdic acid, silicomolybdic acid, phosphotungstic acid, silicotungstic acid, tetraphenylphosphonium bromide, methyltriphenylphosphonium bromide, ethyltriphenylphosphonium bromide, iodine, carbon disulfide) were of reagent grade, received from commercial sources and used as received. Deionized water was used throughout the synthesis. Fourier transform infrared spectra (FT-IR) of the solid samples were recorded at room temperature in the range of 400–4000 cm^{-1} on a Shimadzu FT-IR spectrophotometer. Room temperature powder X-ray diffraction patterns for the solid samples were measured on a Rigaku Powder X-ray diffractometer, Miniflex-600 equipped with a Cu Kα radiation source (λ = 1.540 Å) operating in Bragg–Brentano geometry. The solution state UV-visible spectroscopic experiments were conducted on a Shimadzu UV 2600 UV-vis spectrophotometer in the wavelength range of 200–800 nm. The field emission scanning electron microscope (FESEM) imaging was carried out on a Carl Zeiss model Ultra 55 microscope. EDX spectra were recorded using Oxford Instruments X-Max^N SDD (50 mm^2) systems and INCA software analysis. The images were recorded for solid samples deposited as a very fine film on the surface of carbon tape. The transmission electron microscope (TEM) images were recorded on a JEOL 2100F instrument. The TEM sample was prepared by dispersion of the solid sample in water followed by sonication for 30 minutes. The sonicated suspension was coated on the TEM copper grid through drop casting followed by drying at room temperature. The TGA data was recorded on a Mettler Toledo TGA 1 instrument for the temperature range of 25–700 °C at the rate of 5 °C min^{-1} under an inert flow of dry N_2 gas (flow rate 20 cm^3 min^{-1}). The room temperature NMR spectra were recorded on a Bruker Avance III (500 MHz). The NMR data were recorded in d_6-DMSO solvent. Chemical shifts are indicated as δ values with respect to TMS which is used as an internal standard. The specific surface area measurements were performed by Brunauer–Emmett–Teller (BET) method using Quantachrome Autosorb-ICTCD analyzer. The atomic force microscopy (AFM) experiments were carried out with oxford instruments and the relevant data were analysed by asylum software. The Kelvin probe force microscopy (KPFM) technique was performed in non-contact mode of operation using conductive probe. The conductive probe was coated with Ti/Ir tip with radius of 25 nm, having a spring constant of 2 N m^{-1} and the bias of +3 V was applied to the tip.

Synthesis of compounds 1–9

An aqueous solution of the Keggin $[XM_{12}O_{40}]^{n-}$ (X = P, Si; M = Mo, W) (0.42 mmol in 75 mL) was prepared. To it, 25 mL aqueous–methanolic (4 : 1 v/v) or aqueous solution of phosphonium cation ($RPPh_3$; R = Me, Et, Ph) (3.5 mmol) salt was added. The obtained suspension was refluxed for two hours at 100 °C. The resultant polycrystalline precipitate was washed with water and vacuum dried. Yield: 85–90%.

CH analysis data, observed (calculated): compound **1**: % C, 32.45 (30.44), % H, 2.52 (2.13); compound **2**; % C, 27.67 (26.72), %H, 2.33 (2.24); compound **3**: % C, 26.36 (25.79), % H, 2.038 (2.054); compound **4**: % C, 37.06 (36.29), %H, 2.47 (2.54); compound **5**: % C, 33.07 (32.19), %H, 2.63 (2.707); compound **6**: % C, 31.54 (31.16), %H, 2.47 (2.48); compound **7**: % C, 23.63 (22.19), %H, 1.55 (1.78); compound **8**: % C, 19.17 (19.42), %H, 1.45 (1.63); compound **9**: % C, 28.12 (27.17), %H, 1.95 (1.91).

Result and discussion

The concept of self-organization of organic surfactants has been utilized to design ordered porous materials out of systems which otherwise remain unstructured such as silica type materials.[63] This idea has been extended to inorganic entities to fabricate long range order ensembles. Among the many available candidates for the generation of self-assembled functional materials, nano-sized POMs have been employed as building blocks for the construction of 1D, 2D and 3D supramolecular architectures.[64–67] The self-assemblies of the POM building blocks have been observed majorly in three categories of compounds: (1) the giant POM clusters such as Mo_{154}, Mo_{132} and $Mo_{72}Fe_{30}$ which self-assemble to spherical blackberry structures having hollow interiors, investigated by Liu, Kegel and Müller and their co-workers;[32,68–76] (2) research groups of

Wei, Gouzerh, Cronin and Peng reported self-assemblies of POM nanoclusters covalently grafted with organic ligands;[77–84] and (3) self-assemblies of POM nanohybrids obtained by cation exchange between POM and organic compounds.[2–6,85–88] In the past two decades, efforts have been devoted to the synthesis of assembled structures of POMs in the forms of wires, tubes, vesicles among the many others.[28,89–92] The approach of obtaining assembled architectures from non-covalently modified POMs is thought to be versatile as it encompasses an extensive range of POMs.[93] It is also supposed that this technique allows for the controlled generation of assemblies in terms of their shapes and sizes. Furthermore, the inorganic–organic hybrid compounds, synthesized in this manner, are stabilized by non-covalent electrostatic interactions between the POM anion and organic cation. These building blocks then direct the self-assembly reaction in appropriate solvent, resulting in solid state functional materials. Research groups of Kurth, Wu and Liu reported POM integrated materials wherein the POM surfaces have been altered by surfactants resuting in formation of assemblies of surfactant encapsulated POMs (SEPs).[36,37,93–97] Bio-compatible self-assemblies have also been synthesized by utilizing peptide or protein building blocks.[98] Isolation of well formed POM assembled hybrid structures have also been realized by using bulky organic cations, such as, alkylammonium cations apart from the imidazole and pyridine derivatives,[13,29,99] although reports related to phosphonium cations are rare. These cations facilitate the stacking of the POM building units around them in well defined morphologies rather than into uncharacterized aggregations. Moreover, self-assemblies of different morphologies are displayed depending on the type of electrostatic interactions operating between the POM anion and the cation as well as the manner by which they arrange.[99]

Keggin-based porous materials of the type $[RPPh_3]_n[XM_{12}O_{40}]$ (**1–9**) were synthesized by mixing aqueous solution of POM anions with aqueous–methanolic solution of the phosphonium salts (Scheme 1). Refluxing the precipitate obtained on mixing the two solutions resulted in the desired product. Nine corresponding compounds of this series have been synthesized, namely $[PPh_4]_3[PMo_{12}O_{40}]$ (**1**), $[EtPPh_3]_3[PMo_{12}O_{40}]$ (**2**), $[MePPh_3]_3[PMo_{12}O_{40}]$ (**3**), $[PPh_4]_4[SiMo_{12}O_{40}]$ (**4**), $[EtPPh_3]_4[SiMo_{12}O_{40}]$ (**5**), $[MePPh_3]_4[SiMo_{12}O_{40}]$ (**6**), $[PPh_4]_3[PW_{12}O_{40}]$ (**7**), $[MePPh_3]_3[PW_{12}O_{40}]$ (**8**) and $[PPh_4]_4[SiW_{12}O_{40}]$ (**9**).

The FT-IR plots for compounds **1–9** (Fig. 1) show the bands corresponding to the phosphonium cation (~1483 (s, ν_{as} (C=C)), 1107 (s, ν_s (P–C)), 687 (s, ν(C–H)) and the signature peaks of the Keggin anions (~1064 (m, ν_{as} (PO_4)) in compounds **1–3** and **7–8** and ~910 (m, ν_{as}(SiO_4)) in compounds **4–6** and **9**, which confirm the presence of both the entities in the hybrid porous materials.[100]

The powder XRD patterns recorded (in the range 2θ = 5–40°) for the hybrid compounds **1–9** are shown in Fig. 2(a). The PXRD plots show a peak in the region 2θ = 7–10° (d ~1.2 nm) which is characteristic of the Keggin structure.[101] The phases and structures of compounds **1–9** have also been investigated by recording their XRD patterns and compared with those of their parent

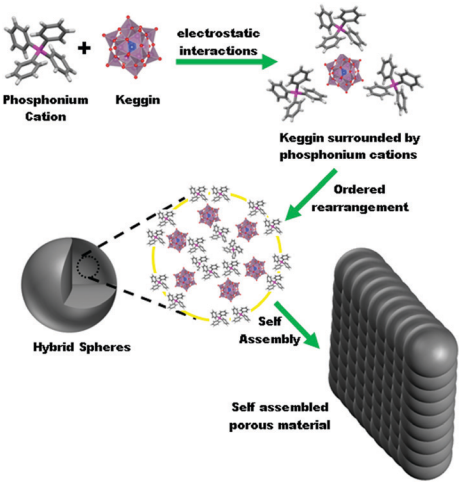

Scheme 1 Schematic representation for the self-assembly route to mesoporous materials (**1–9**) through electrostatically held hybrid spherical aggregates of Keggin anions and phosphonium cations.

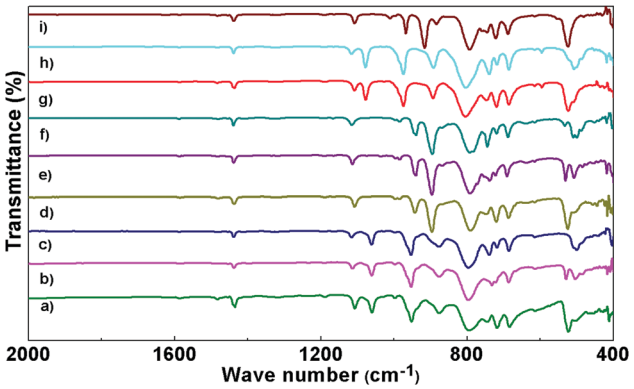

Fig. 1 Comparative IR spectra for (a) compound **1**; (b) compound **2**; (c) compound **3**; (d) compound **4**; (e) compound **5**; (f) compound **6**; (g) compound **7**; (h) compound **8**; (i) compound **9**.

Keggin compounds (Fig. 2(b)). While the hybrid compounds show a very broad feature in the wide angle region of 2θ = 15–40°, the respective Keggin compounds show a number of Bragg peaks in the same region. The PXRD pattern of the hybrid compounds is relatively different from the Keggin compounds, which indicate that the secondary structures of the Keggin derivatives (compounds **1–9**) are influenced by the presence and nature of cations.

Compounds **1–9** obtained as polycrystalline precipitate were imaged using FESEM (Fig. 3). A thin layer of the compound was coated on the surface of a carbon tape prior to recording the data. The FESEM images show coral (elongated spherical structures) shaped assemblies[38] with sizes ranging from 100–200 nm. The energy dispersive X-ray (EDX) spectroscopy shows the presence of carbon, phosphorous (or silicon) and molybdenum (or tungsten) throughout the assemblies signifying the presence of both the Keggin anion and the phosphonium cation (ESI,† Fig. S6). The FESEM images for compounds **1–9**

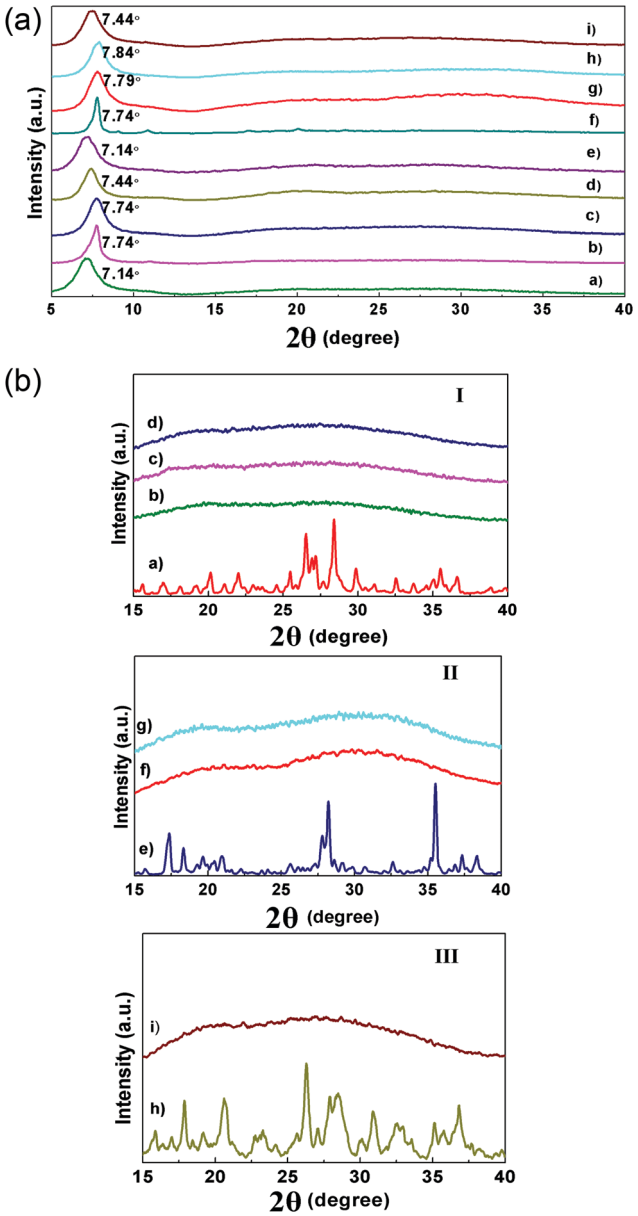

Fig. 2 Comparative PXRD spectra for (a) compound **1**; (b) compound **2**; (c) compound **3**; (d) compound **4**; (e) compound **5**; (f) compound **6**; (g) compound **7**; (h) compound **8**; (i) compound **9**. Fig. 2b. Wide angle XRD spectra for the POM hybrid materials and their parent Keggin; I (a) $H_3[PMo_{12}O_{40}]$; (b) compound **1**; (c) compound **2**; (d) compound **3**; II (e) $H_3[PW_{12}O_{40}]$; (f) compound **7**; (f) compound **8**; III (h) $H_4[SiW_{12}O_{40}]$; (i) compound **9**.

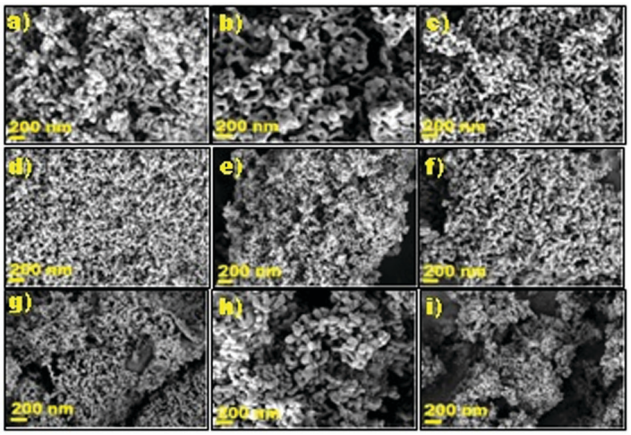

Fig. 3 FESEM images for (a) compound **1**; (b) compound **2**; (c) compound **3**; (d) compound **4**; (e) compound **5**; (f) compound **6**; (g) compound **7**; (h) compound **8**; (i) compound **9**.

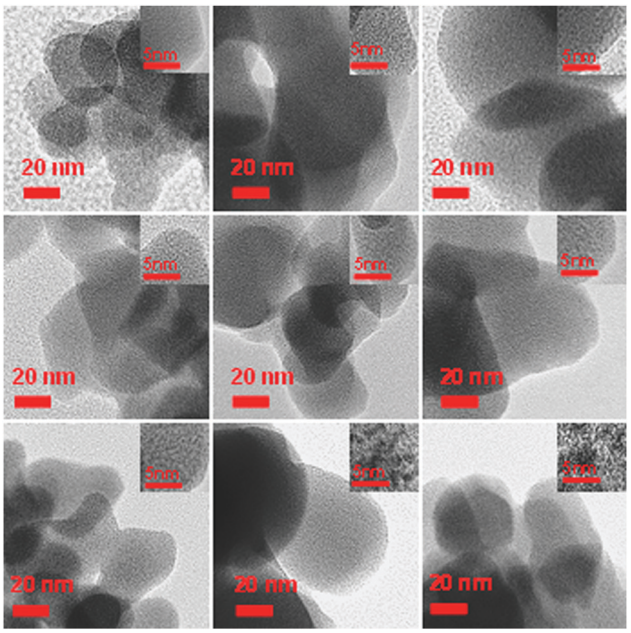

Fig. 4 TEM images for (a) compound **1**; (b) compound **2**; (c) compound **3**; (d) compound **4**; (e) compound **5**; (f) compound **6**; (g) compound **7**; (h) compound **8**; (i) compound **9**. The inset shows the HR-TEM image for the respective compound.

also show the presence of inner channel and cavities (organized unevenly) which is most probably the reason for the evident porosity in these compounds.

Compounds **1–9** were also imaged using the TEM technique. The samples were prepared by sonicating aqueous suspension of the compounds (1.5 mg mL^{-1}) for 30 minutes. The resultant suspensions were drop casted on copper grids and allowed to dry prior to the recording of the TEM data. The TEM images, obtained for compounds **1–9** (Fig. 4), exhibit spherical aggregates with average diameter of ~20 nm. The most characteristic feature of the high resolution TEM (HR-TEM) images, obtained, is the granular appearance of the hybrid colloidal spherical aggregates, which give an impression of small highly contrasting dots, embedded within a poorly electron contrasting substance. While the small black dots denote the Keggin polyanion, the low contrasting material corresponds to the phosphonium cations surrounding the polyanion.[38,98] The mesoporous compounds **1–9** display high thermal stability showing disintegration only beyond 300 °C as confirmed from their thermogravimetrical analyses (ESI,† Fig. S9, S10a–i). The porous nature of compounds **1–9** was investigated by nitrogen

sorption experiments (ESI,† Fig. S13). The hybrid compounds show type IV nitrogen adsorption–desorption isotherm with H_1-type hysteresis loop[39] in the relative pressure range p/p_o of 0.9 to 1.0 indicating the formation of mesoporous compounds. The H_1-type hysteresis loop suggests a fairly uniform arrangement of spherical agglomerates with cylindrical pore geometry. This outcome is in accordance with the proposed aggregation of spherical particles leading to mesoporous material.

The specific surface area measurements for compounds **1–9** show the presence of pores with an average size of 32.9 nm and pore volume of 0.38 $cm^3\ g^{-1}$. Therefore, compounds **1–9** can be classified as mesoporous compounds with an average surface area of $\sim$25 $m^2\ g^{-1}$. Since it is known that bare hetero polyanions (HPAs), generally exhibit low surface areas, it can be said that the cations play an important role in the synthesis of mesoporous materials as it is their arrangement around the Keggin moiety (as directed by the non-covalent interactions) and the further aggregation of the spherical agglomerates that provide them their porosity.

The Keggin anion $[PM_{12}O_{40}]^{3-}$ (or $[SiM_{12}O_{40}]^{4-}$ M = Mo, W) of the mesoporous compounds **1–9** (which are hybrid self-assemblies of Keggin anion and phosphonium cation) can be envisaged as the tetrahedral ion, PO_4^{3-} (or SiO_4^{4-}) held within a $\{M_{12}O_{36}\}$ cage.[5] In the porous compounds of the type $[RPPh_3]_n[XM_{12}O_{40}]$, the organic cations are therefore sufficiently attracted (*via* electrostatic interactions) to the central tetrahedral anion, the two being separated by the $\{M_{12}O_{36}\}$ cage. The Keggin anions and the phosphonium cations, which are randomly oriented in the aqueous solution, reorganize/rearrange themselves in such a way that the phosphonium cations, which are hydrophobic and non-covalently bound to the Keggin, lie on the surface of the Keggin molecule. This orientation of the phosphonium cations on the Keggin surface serves as the base for the formation of hybrid spherical aggregates of $[RPPh_3]_n[XM_{12}O_{40}]$ as observed in the TEM images (Fig. 4). Further, it is expected that the observed porosity in the compounds **1–9** arises during the arrangement of spherical aggregates which results in the formation of inner channels and cavities which are unevenly distributed throughout the Keggin-based mesoporous compounds. Consequently, the hydrophobicity of the pores can be attributed to the phenyl rings of the organic cations which line the pore surface.

We also studied the surface potential measurements by using Kelvin probe force microscopy (KPFM) technique. The concerned images are given in the ESI† (Fig. S23–S26). We could perform surface potential measurements of five representative samples (compounds **1**, **2**, **4**, **7** and **9**) out of nine samples described in this work. Compounds **1**, **2** and **4** are molybdenum containing Keggin associated self assembly and compounds **7** and **9** are tungsten containing Keggin associated assembly. As shown from the KPFM images, the tungsten compounds $[PPh_4]_3[PW_{12}O_{40}]$ (**7**) and $[PPh_4]_4[SiW_{12}O_{40}]$ (**9**) show negative surface potentials. On the contrary, the molybdenum compounds $[PPh_4]_3[PMo_{12}O_{40}]$ (**1**), $[EtPPh_3]_3[PMo_{12}O_{40}]$ (**2**) and $[PPh_4]_4[SiMo_{12}O_{40}]$ (**4**) exhibit positive surface potentials. It is evident from the observed data that the cation components of the compounds do not play any major role on the nature (whether positive or negative) of observed surface potentials of the materials, because both compounds **7** and **9** have same cationic entity.

In the case of tungsten containing compounds **7** and **9**, the negative surface potential implies that the negative charges of the surface POM anions are not fully counterbalanced by the surface phosphonium cations in the interface between the phosphonium cation and POM anion. This may be due to the kinetic sluggishness of tungsten (in comparison to molybdenum). On the same logic, in case of molybdenum compounds, **1**, **2** and **4**, the positive surface potential indicates that the net positive charges of the surface phosphonium cations are not completely counterbalanced by the net negative charges of the surface POM anions in the interface of phosphonium cation and POM anion.

The porosity and thermal stability of inorganic–organic hybrid materials **1–9** encouraged us to explore the adsorption/uptake of certain environmentally malignant molecules. The choice of the guest was chiefly driven by the fact that the phosphonium cations of the hybrid porous compounds are present on the exterior of the pore walls which render them hydrophobic in nature. Therefore, guests with complimenting nature are welcome. Apart from the hydrophobic character of the incoming molecule, it is observed that its size and shape are also important. The porous materials were applied for the adsorption of three guests: iodine (I_2), toxic carbon disulfide (CS_2) and non-degrading methyl orange dye. It was found that while the porous materials readily adsorbed guests such as I_2 and CS_2, they were unable to adsorb methyl orange dye which was rejected because of its bulky size and non-linear shape. Hence, it can be said that the porous materials, apart from exhibiting selectivity in terms of the nature of the incoming guest, also display selective adsorption, based on the shape and size of the guest.

Iodine adsorption studies

In order to explore the reversible iodine (I_2) adsorption and release ability of compounds **1–9**, fresh samples of the compounds (25 mg) were exposed to iodine vapours (1 g) in a gas–solid reaction at room temperature and were monitored in real time. The mesoporous compounds **1–9**, on exposure to I_2 showed a gradual colour change from yellow (compounds **1–6**) or white (compounds **7–9**) to brown with time (Scheme 2).

The brown colour of the porous materials, observed due to the adsorption of I_2, intensified till 15 days, after which no further colour change was observed indicating the saturation of I_2 uptake by the porous compounds. This observation was also supported by the time dependent UV-visible studies, conducted for compound **1** which showed gradual increase in the uptake of iodine, saturating after 15 days, after which minimal increase in the adsorption of I_2 was observed (Fig. 5 and Table S4, ESI†). The adsorbed I_2 could be easily removed by the simple immersion of the I_2-loaded hybrid POM compounds in organic solvents such as ethanol and hexane.

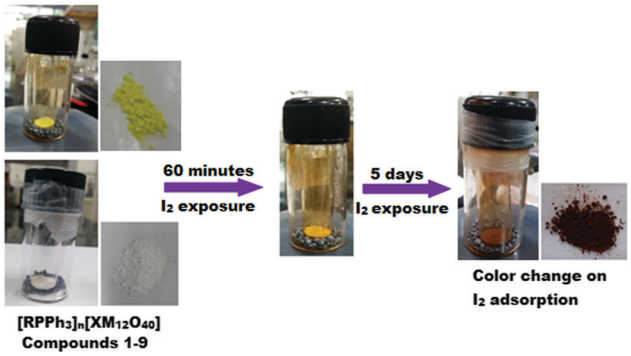

Scheme 2 Real time adsorption of I_2 by compounds **1–9**.

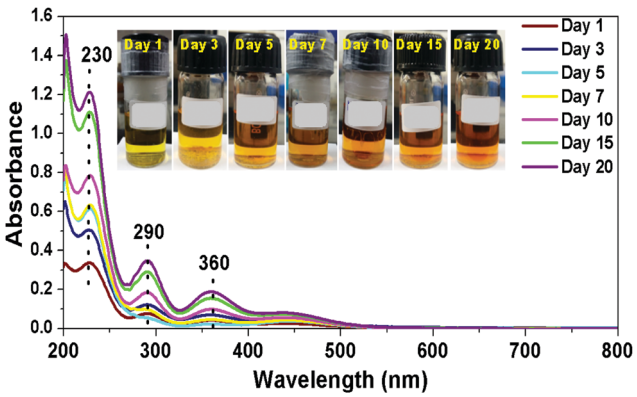

Fig. 5 UV-visible spectra of ethanol solutions containing iodine extracted from compound **1** at different intervals of time.

On immersion, I_2 leached from the mesoporous compounds into ethanol (brown coloration) or hexane (violet coloration). Powdered compounds **1–9** themselves showed a colour change from brown to yellow (or white) after 3–4 hours of immersion confirming the removal of adsorbed I_2. The structural integrity of the compounds post I_2 uptake and its removal was confirmed by IR spectroscopy (ESI,† Fig. S2a and b). Since the POM integrated hybrid materials exhibit easy uptake and release of I_2 they can act as suitable candidates for capturing radioactive I_2 thereby helping in nuclear waste management.

The quantification of the amount of I_2 adsorbed by the porous materials **1–9** was carried out by the method of linear correlation in accordance with the Lambert Beer's Law (ESI,† Fig. S14–S17 and Tables S2, S5). The extraction of the adsorbed I_2 by compounds **1–9** was carried out both in ethanol and hexane and the obtained solutions were analyzed by UV-visible spectroscopy for their capturing ability of I_2 (Fig. 6 and ESI,† Fig. S18).

The UV-visible analysis showed that compounds **1–9** adsorbed variable amounts of I_2. The highest I_2 adsorption capacity in ethanol for the mesoporous compounds under study was measured as 1.03, 0.98 and 0.95 mg of I_2/(mg of the porous compound) for compounds **5**, **4** and **1**, respectively (ESI,† Table S3). The controlled experiments show that the

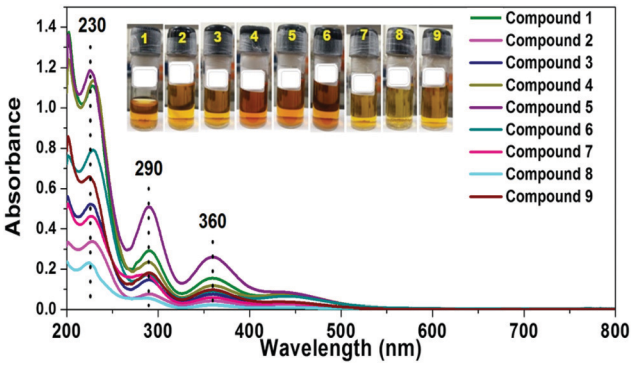

Fig. 6 Solution state UV-Visible spectra for extracted iodine solutions of compounds **1–9** in ethanol. The solutions were diluted 50 times prior to recording of the data.

iodine adsorption is facilitated by the phosphonium components of the titled hybrid materials (see ESI† for the the details).[102] Four cycles of reversible adsorption and desorption of I_2 were carried out for compound **1**. The amount of adsorbed I_2 varied from 0.90 mg to 0.75 mg of I_2/(mg of compound **1**) for cycle 1 and 3 and remained constant thereafter (ESI,† Fig. S19 and Table S7).

We have conducted iodine adsorption by the constituent protonated salt of Keggin anions and phosphonium cations (as bromide salts) as controlled experiments. The phosphomolybdic acid, silicomolybdic acid, phosphotungstic acid and silicotungstic acid, as such do not adsorb iodine but the phosphonium salts adsorb iodine. These experiments clearly suggest that the phosphonium part of the obtained self-assembled materials plays important role for the iodine adsorption in the present work. Even though, the phosphonium bromide salt adsorbs iodine, this cannot be compared to the iodine adsorption by self-assembled materials in the present study, because phosphonium bromide salt is a molecular level (water soluble) substance, not a heterogeneous material.

Another choice of suitable guest was CS_2 but due to its toxic nature, its reversible adsorption studies by the porous compounds was limited to $[PPh_4]_3[PMo_{12}O_{40}]$ (**1**). When exposed to CS_2 vapours, compound **1** showed a visible colour change from yellow to green. The green colour of the compound intensified with continuous exposure to CS_2 vapours for one week (Scheme 3). The adsorption of CS_2 by porous compound **1** can be explained on the basis of strong electrostatic interaction (in the form of quadrupole interactions) between the phenyl ring of the phosphonium cation and the incoming CS_2

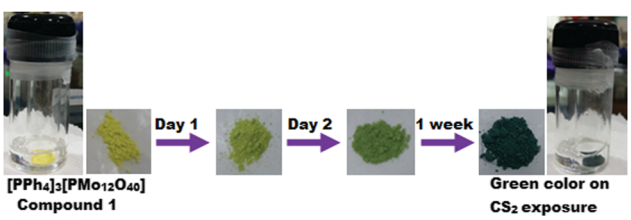

Scheme 3 Time dependent CS_2 adsorption by compound **1**.

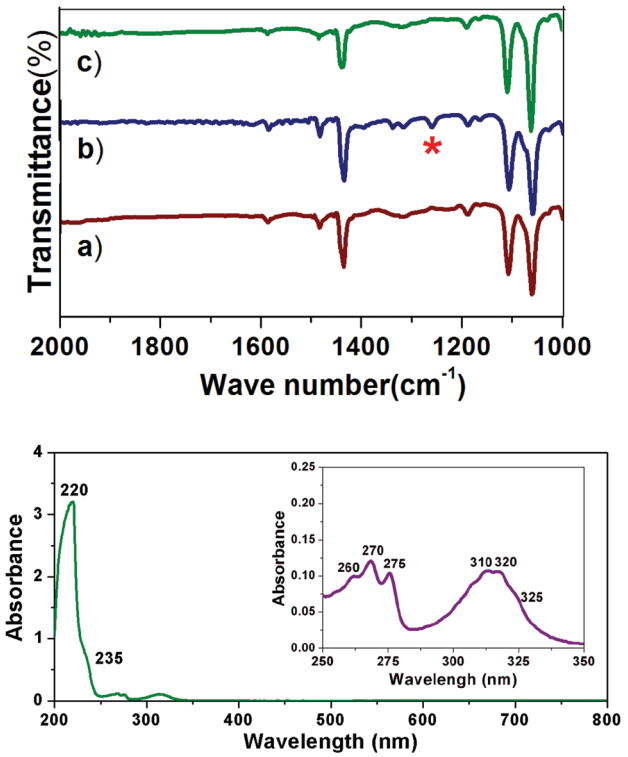

Fig. 7 (I) IR spectra of (a) compound **1**; (b) compound **1** exposed to CS_2 vapours; (c) regenerated compound **1** obtained from methanol; (II) UV-visible spectrum for compound **1**; inset: enlarged view of the spectrum in the UV range 250–350 nm.

molecule. The adsorbed CS_2 was easily removed from the CS_2-loaded compound **1** by its extraction in methanol. As the adsorbed CS_2 leached into methanol, compound **1** gradually changed color from green to yellow, the complete desorption taking place in 3–4 hours. Compound **1** showed no structural disintegration during the uptake and removal of CS_2 as confirmed by IR spectroscopy (Fig. 7) The successful adsorption of CS_2 within the pores of compound **1** was confirmed by IR, UV-visible and NMR spectroscopy (ESI,† Fig. S21). The IR spectra of the CS_2 loaded compound **1** showed a band at 1265 cm^{-1} corresponding to C═S stretch originally absent in compound **1**.[103] Additionally, the UV-visible spectrum for the methanolic solution of CS_2 shows an intense peak at 220 nm and weak bands in the range of 230–330 nm in the UV region of the spectrum confirming presence of CS_2 (Fig. 7).[104]

Three cycles of reversible uptake and removal of CS_2 by compound **1** were performed which showed minimal decline in its efficiency for adsorption of CS_2 after each cycle (ESI,† Fig. S22). Therefore the POM incorporated mesoporous compounds **1–9** can act as suitable hosts for the selective capture of linear non-polar molecules such as radioactive I_2 and CS_2 which are environment unfriendly.

Conclusions

In summary, a series of mesoporous Keggin-based hybrid materials have been successfully synthesized and characterized. The synthesis of the hybrid materials in the present study is an example of non-covalent functionalization of POMs involving cation replacement reaction of POMs. The anion and the phosphonium cation in the porous material are held together by non-covalent interactions. In contrast to the commonly used surfactants and ammonium cations, phosphonium cations have been utilized as the counter cations in the ion exchange reaction. In the solution phase, the randomly oriented, closely associated Keggin anion and phosphonium cation form spherical aggregates, with the phosphonium cations present on the Keggin surface. The porosity of these materials is the result of the self assembling tendency of the polyanion and the bulkier tetraphenylphosphonium cation. Since these compounds efficiently adsorb I_2 and CS_2 on their surfaces, we propose that these porous hybrids serve to selectively and reversibly adsorb non-polar linear molecules, tentatively due to the hydrophobic interactions between the phenyl moities of cation and the guest molecules. This piece of work therefore, highlights the role of the cation in directing the self-assemblies offering new prospects, wherein diverse POM self-assemblies can be generated by employing different cations (both lipophillic and lipophobhic). Furthermore, the surface properties can be modulated by choosing appropriate cations, which fit best to the desired requirements.

Author contributions

The manuscript was written through contributions of all authors. All authors have given approval to the final version of the manuscript.

Conflicts of interest

There are no conflicts to declare.

Acknowledgements

We thank SERB, DST, government of India with project number (SB/EMEQ-090/2014) for the financial support. The financial grant from UPE-II (project No. 58), DST-PURSE and DST-FIST are gratefully acknowledged. KT thanks CSIR for fellowship. We thank AIRF an instrumentation facility at JNU. We thank Prof. Akhilesh Verma and Dr. Sasanka Deka for elemental analysis data.

References

1 P. M. Sivakumar, V. I. Kodolov, G. E. Zaikov and A. K. Haghi, Self-assembly of nanostructures: Nanostructure, nanosystem and nanostructured materials, in *nanostructure, nanosystem and nanostructured materials: Theory, product and development Eds.*, Springer, Berlin, Germany, 2005, pp. 438–460.
2 M. Clemente-León, E. Coronado, C. J. Gómez-Gareía, C. Mingotaud, S. Ravaine, G. Romualdo-Torres and P. Delhaès, Polyoxometalate monolayers in Langmuir–Blodgett films, *Chem. – Eur. J.*, 2005, **11**, 3979–3987.

3 S. Q. Liu, H. Möhwald, D. Volkmer and D. G. Kurth, Polyoxometalate based electro- and photochromic dual-mode devices, *Langmuir*, 2006, **22**, 1949–1951.
4 T. Ito, H. Yashiro and T. Yamase, Regular two-dimensional molecular array of photoluminescent Anderson type polyoxometalate constructed by Langmuir–Blodgett technique, *Langmuir*, 2006, **22**, 2806–2810.
5 H. Li, H. Sun, W. Qi, M. Xu and L. Wu, Onion like hybrid assemblies based on surfactant encapsulated polyoxometalates, *Angew. Chem., Int. Ed.*, 2007, **46**, 1300–1303.
6 S. Liu and Z. Tang, Polyoxometalate based functional nanostructured films: Current progress and future prospects, *Nano Today*, 2010, **5**, 267–281.
7 W. Li, W. Bu, H. Li, L. Wu and M. A. Li, surfactant-encapsulated polyoxometalate complex towards a thermotropic liquid crystal, *Chem. Commun.*, 2005, 3785–3787.
8 C. Jahier, M. Cantuel, N. D. McClenaghan, T. Buffeteau, D. Cavagnat, F. Agbossou, M. Carraro, M. Bonchio and S. Nlate, Enantiopure dendritic polyoxometalates: Chirality transfer from dendritic wedges to a POM cluster for asymmetric sulfide oxidation, *Chem. – Eur. J.*, 2009, **15**, 8703–8708.
9 A. Nisar, J. Zhuang and X. Wang, Construction of amphiphilic polyoxometalate mesostructures as a highly, efficient desulfurization catalyst, *Adv. Mater.*, 2011, **23**, 1130–1135.
10 Y. Wang, H. Li, W. Qi, Y. Yang, Y. Yan, B. Li and L. Wu, Supramolecular assembly of chiral polyoxometalate complexes for asymmetric catalytic oxidation of thio ethers, *J. Mater. Chem.*, 2012, **22**, 9181–9188.
11 S. I. Stupp, V. Le Bonheur, K. Walker, L. S. Li, K. E. Huggins, M. Keser and A. Amstutz, Supramolecular Materials: Self-organized nanostructures, *Science*, 1997, **276**, 384–389.
12 D. B. Amabilino, D. K. Smith and J. W. Steed, Supramolecular materials, *Chem. Soc. Rev.*, 2017, **46**, 2404–2420.
13 C. Tan, Self-assembly, aggregates morphology and ionic liquid crystals of polyoxometalate-based hybrid molecule: From vesicles to layered structure, *J. Mol. Struct.*, 2017, **1148**, 34–39.
14 A. Proust, R. Thouvenot and P. Gouzerh, Functionalization of polyoxometalates: Towards advanced applications in catalysts and materials science, *Chem. Commun.*, 2008, 1837–1852.
15 B. Zhang, P. Yin, F. Haso, L. Hu and T. Liu, Soft matter approaches for enhancing the catalytic capabilities of polyoxometalate clusters, *J. Cluster Sci.*, 2014, **25**, 695–710.
16 Y. Yan, H. Wang, B. Li, G. Hou, Z. Yin, L. Wu and W. W. Yam, Smart self-assemblies based on a surfactant-encapsulated photoresponsive polyoxometalate complex, *Angew. Chem., Int. Ed.*, 2010, **49**, 9233–9236.
17 Y. Yang, Y. Wang, H. Li, W. Li and L. Wu, Self-assembly and structural evolvement of polyoxometalate-anchored dendron complexes, *Chem. – Eur. J.*, 2010, **16**, 8062–8071.
18 Y. Yang, L. Yue, H. Li, E. Maher, Y. Li, Y. Wang, L. Wu and V. W.-W. Yam, Photo-responsive self-assembly of an azobenzene-ended surfactant-encapsulated polyoxometalate complex for modulating catalytic reactions, *Small*, 2012, **8**, 3105–3110.
19 D. Chong, J. Tan, J. Zhang, Y. Zhou, X. Wan and J. Zhang, Dual electric switching permeability of vesicles *via* redox-responsive self-assembly of amphiphilic block copolymers and polyoxometalates, *Chem. Commun.*, 2018, **54**, 7838–7841.
20 A. B. Bourlinos, K. Raman, R. Herrera, Q. Zhang, L. A. Archer and E. P.-A. Giannelis, liquid derivative of 12-tungstophosphoric acid with unusually high conductivity, *J. Am. Chem. Soc.*, 2004, **126**, 15358–15359.
21 Y. Leng, J. Wang, D. Zhu, X. Ren, H. Ge and L. Shen, Heteropolyanion based ionic liquids: Reaction-induced self-separation catalysts for esterification, *Angew. Chem., Int. Ed.*, 2008, **48**, 168–171.
22 H. Li, Y. Qiao, L. Hua, Z. Hou, B. Feng, Z. Pan, Y. Hu, X. Wang, X. Zhao and Y. Yu, Imidazolium polyoxometalate: An ionic liquid catalyst for esterification and oxidative esterification, *ChemCatChem*, 2010, **2**, 1165–1170.
23 B. Zhen, H. Li, Q. Jiao, Y. Li, Q. Wu and Y. Zhang, $SiW_{12}O_{40}$-based ionic liquid catalysts: Catalytic esterification of oleic acid for biodiesel production, *Ind. Eng. Chem. Res.*, 2012, **51**, 10374–10380.
24 Y. Li, X. Wu, Q. Wu, H. Ding and W. Yan, Reversible phase transformation ionic liquids based on ternary Keggin polyoxometalates, *Ind. Eng. Chem. Res.*, 2014, **53**, 12920–12926.
25 W. Li and L. Wu, Hybrid liquid crystals from the self-assembly of surfactant-encapsulated polyoxometalate complexes, *Chin. J. Chem.*, 2015, **33**, 15–23.
26 C. Li, Z. Jiang, J. Gao, Y. Yang, S. Wang, F. Tian, F. Sun, X. Sun, P. Ying and C. Hand, Ultra-deep desulfurization of diesel: Oxidation with a recoverable catalyst assembled in emulsion, *Chem. – Eur. J.*, 2004, **10**, 2277–2280.
27 H. Lü, J. Gao, Z. Jiang, F. Jing, Y. Yang, G. Wang and C. Li, Ultra-deep desulfurization of diesel by selective oxidation with $[C_{18}H_{37}N(CH_3)_3]_4[H_2NaPW_{10}O_{36}]$ catalyst assembled in emulsion droplets, *J. Catal.*, 2006, **239**, 369–375.
28 W. Bu, S. Uchida and N. Mizuno, Micelles and vesicles formed by polyoxometalate-block copolymer composites, *Angew. Chem., Int. Ed.*, 2009, **48**, 8281–8284.
29 L. Leclercq, A. Mouret, S. Renaudineau, V. Schmitt, A. Proust and V. Nardello-Rataj, Self-assembled polyoxometalates nanoparticles as pickering emulsion stabilizers, *J. Phys. Chem. B*, 2015, **119**, 6326–6337.
30 A. Wu, X. Gao, L. Liang, N. Sun and L. Zheng, Interaction among worm-like micelles in polyoxometalate-based supramolecular hydrogel, *Langmuir*, 2019, **35**, 6137–6144.
31 N. Lei, L. Feng and X. Chen, Zwitterionic surfactant micelle-directed self-assembly of Eu-containing polyoxometalate into organized nanobelts with improved emission and pH responsiveness, *Langmuir*, 2019, **35**, 4370–4379.
32 M. L. Kistler, A. Bhatt, G. Liu, D. Casa and T. A. Liu, Complete macro ion- ''Blackberry'' assembly-macroion transition with continuously adjustable assembly sizes in $\{Mo_{132}\}$ water/acetone systems, *J. Am. Chem. Soc.*, 2007, **129**, 6453–6460.
33 D. Li, J. Zhang, K. Landskron and T. Liu, Spontaneous self-assembly of metal–organic cationic nanocages to form

monodisperse hollow vesicles in dilute solutions, *J. Am. Chem. Soc.*, 2008, **130**, 4226–4227.

34 P. Yin, D. Li and T. Liu, Solution behaviors and self-assembly of polyoxometalates as models of macroions and amphiphilic polyoxometalate-organic hybrids as novel surfactants, *Chem. Soc. Rev.*, 2012, **41**, 7368–7383.

35 X. Cheng, P. Sun, S. Zhang, D. Sun, B. Jiang, W. Wang and X. Xin, Self assembly of m-phenylenediamine and polyoxometalate into hollow-sphere and core-in-hollow-shell nanostructures for selective adsorption of dyes, *J. Mol. Liq.*, 2019, **287**, 110982.

36 D. Volkmer, A. DuChesne, D. G. Kurth, H. Schnablegger, P. Lehmann, M. J. Koop and A. Müller, Toward nanodevices: Synthesis and characterization of the nanoporous surfactant-encapsulated Keplerate $(DODA)_{40}(NH_4)_2[(H_2O)_n \subset Mo_{132}O_{372}(CH_3COO)_{30}(H_2O)_{72}]$, *J. Am. Chem. Soc.*, 2000, **122**, 1995–1998.

37 D. G. Kurth, P. Lehmann, D. Volkmer, A. Müller and D. Schwahn, Biologically inspired polyoxometalate-surfactant composite materials: Investigations on the structures of discrete, surfactant-encapsulated clusters, monolayers and Langmuir–Blodgett films of $DODA)_{40}(NH_4)_2[(H_2O)_n \subset Mo_{132}O_{372}(CH_3CO_2)_{30}(H_2O)_{72}]$, *J. Chem. Soc., Dalton Trans.*, 2000, **21**, 3989–3998.

38 M. V. Vasylyev and R. Neumann, New heterogeneous polyoxometalate based mesoporous catalysts for hydrogen peroxide mediated oxidation reactions, *J. Am. Chem. Soc.*, 2004, **126**, 884–890.

39 P. Zhao, Y. Zhang, D. Li, H. Cui and L. Zhang, Mesoporous polyoxometalate-based ionic hybrid as a highly effective heterogeneous catalyst for direct hydroxylation of benzene to phenol, *Chin. J. Catal.*, 2018, **39**, 334–341.

40 Y. Guo, Y. Wang, C. Hu, Y. Wang, E. Wang, Y. Zhou and S. Feng, Microporous polyoxometalates POMs/SiO_2: Synthesis and photocatalytic degradation of aqueous organocholorine pesticides, *Chem. Mater.*, 2000, **12**, 3501–3508.

41 G. M. Suppes, B. A. Deore and M. S. Freund, Porous conducting polymer/heteropolyoxometalate hybrid material for electrochemical supercapacitor applications, *Langmuir*, 2008, **24**, 1064–1069.

42 D. Zhou and B. H. Han, Graphene-based mesoporous materials assembled by mediation of polyoxometalate nanoparticles, *Adv. Funct. Mater.*, 2010, **20**, 2717–2722.

43 F. Ma, S. Liu, D. Liang, G. Ren, C. Zhang, F. Wei and Z. Su, Hydrogen adsorption in polyoxometalate hybrid compounds based on porous metal–organic frameworks, *Eur. J. Inorg. Chem.*, 2010, 3756–3761.

44 Y. J. Tang, M. R. Gao, C. H. Liu, S. L. Li, H. L. Jiang, Y. Q. Lan, M. Han and S. H. Yu, Porous molybdenum-based hybrid catalysts for highly efficient hydrogen evolution, *Angew. Chem., Int. Ed.*, 2015, **54**, 12928–12932.

45 D. Y. Du, J. S. Qin, S. L. Li, Z. M. Su and Y. Q. Lan, Recent advances in porous polyoxometalate-based metal–organic framework materials, *Chem. Soc. Rev.*, 2014, **43**, 4615–4632.

46 Y. Zhou, G. Chen, Z. Long and J. Wang, Recent advances in polyoxometalate-based heterogeneous catalytic materials for liquid-phase organic transformations, *RSC Adv.*, 2014, **4**, 42092–42113.

47 E. Naseri and R. Khoshnavazi, Sandwich type polyoxometalates encapsulated into the mesoporous material: Synthesis, characterization and catalytic application in the selective oxidation of sulphides, *RSC Adv.*, 2018, **8**, 28249–28260.

48 Y. Guo, Y. Yang, C. Hu, C. Guo, E. Wang, Y. Zou and S. Feng, Preparation, characterization and photochemical properties of ordered macroporous hybrid silica materials based on monovacant Keggin-type polyoxometalates, *J. Mater. Chem.*, 2002, **12**, 3046–3052.

49 V. Dufaud and F. Lefebvre, Inorganic hybrid materials with encapsulated polyoxometalates, *Materials*, 2010, **3**, 682–703.

50 F. Su, L. Ma, Y. Guo and W. Li, Preparation of ethane-bridged organosilica group and Keggin type heteropoly-acid co-functionalized ZrO_2 hybrid catalyst for biodiesel synthesis from erucasatira gars oil, *Catal. Sci. Technol.*, 2012, **2**, 2367–2374.

51 F. Su, Q. Wu, D. Song, X. Zhang, M. Wang and Y. Guo, Pore morphology-controlled preparation of ZrO_2-based hybrid catalyst functionalized by both organosilica moieties and Keggin-type heteropoly acid for the synthesis of levulivate esters, *J. Mater. Chem. A*, 2013, **1**, 13209–13221.

52 F. Su, L. Ma, D. Long, X. Zhang and Y. Guo, Design of a highly ordered mesoporous $H_3PW_{12}O_{40}/ZrO_2$-Si(Ph)Si hybrid catalyst for methyl levulinate synthesis, *Green Chem.*, 2013, **15**, 885–890.

53 K. Ishizaki, S. Komareni and M. Nanko, Applications of porous materials, in *Porous materials: Process technology and applications*, Springer, Dordrecht, Boston, 1998, pp. 181–201.

54 G. E. Park and T. J. Webster, Porous materials for biological applications, in *Encyclopedia of medical devices and instrumentation*, ed. J. G. Webster, John Wiley and sons, 2006, pp. 392–406.

55 M. Takahashi and M. Fuji, Synthesis and fabrication of inorganic porous materials: From nanometer to millimetre sizes, *KONA Powder Part. J.*, 2002, **20**, 84–97.

56 X. S. Zhao, F. Su, Q. Yan, W. Gao, X. Y. Bao, L. Lv and Z. Zhou, Templating methods for preparation of porous structures, *J. Mater. Chem.*, 2006, **16**, 637–648.

57 J. A. Martens, J. Jammaer, S. Bajpe, A. Aerts, Y. Lorgouilloux and C. E.-A. Kirschhock, Simple synthesis recipes of porous materials, *Microporous Mesoporous Mater.*, 2011, **140**, 2–8.

58 D. Wu, F. Xu, B. Sun, R. Fu, H. He and K. Matyjaszewski, Design and preparation of porous polymers, *Chem. Rev.*, 2012, **112**, 3959–4105.

59 M. Sun, C. Chen, L. Chen and B. Su, Hierarchically porous materials: Synthesis, strategies and emerging applications, *Front. Chem. Sci. Eng.*, 2016, **10**, 301–347.

60 X. Y. Yang, L. H. Chen, Y. Li, J. C. Rooke, C. Sancher and B. L. Su, Hierarchically porous materials: Synthesis strategies and structure design, *Chem. Soc. Rev.*, 2017, **46**, 481–558.

61 T. J. Barton, L. M. Bull, W. G. Klemperer, D. A. Loy, B. McEnaney, M. Misono, P. A. Monson, G. Pez, G. W. Scherer, J. C. Vartuli and O. M. Yaghi, Tailored porous materials, *Chem. Mater.*, 1999, **11**, 2633–2656.

62 J. S. Beck, J. C. Vartuli, N. J. Roth, M. E. Leonowicz, C. T. Kresge, K. D. Schmitt, C. T.-W. Chu, D. H. Olson, E. W. Sheppard, S. B. McCullen, J. B. Higgins and J. L. Schlenker, A new family of mesoporous molecular sieves prepared with liquid crystal templates, *J. Am. Chem. Soc.*, 1992, **114**, 10834–10843.

63 M. Zeng, J. Tan, K. Chen, D. Zang, Y. Yang, J. Zhang and Y. Wei, Guest controlled pillar [5]arene and polyoxometalate based two-dimensional nanostructures toward reversible iodine capture, *ACS Appl. Mater. Interfaces*, 2019, **11**, 8537–8544.

64 S. Polarz, B. Smarsly and M. Antonietti, Colloidal organization and clusters: Self-assembly of polyoxometalate-surfactant complexes towards three-dimensional organized structures, *ChemPhysChem*, 2001, **2**, 457–461.

65 T. Zhang, J. Brown, R. J. Oakley and C. F.-J. Faul, Towards functional nanostructures: Ionic self-assembly of polyoxometalates and surfactants, *Curr. Opin. Colloid Interface Sci.*, 2009, **14**, 62–70.

66 P. Yin, A. Bayaguud, P. Cheng, F. Haso, L. Hu, J. Wang, D. Vezenov, R. E. Winans, J. Hao, T. Li, Y. Wei and T. Liu, Spontaneous stepwise self-assembly of a polyoxometalate-organic hybrid into catalytically active one-dimensional anisotropic structures, *Chem. – Eur. J.*, 2014, **20**, 9589–9595.

67 C. Li, N. Mizuno, K. Yamaguchi and K. Suzuki, Self-assembly of anionic polyoxometalate-organic architectures based on lacunary phosphomolybdates and pyridyl ligands, *J. Am. Chem. Soc.*, 2019, **141**, 7687–7692.

68 T. Liu, Supramolecular structures of polyoxomolybdate-based giant molecules in aqueous solution, *J. Am. Chem. Soc.*, 2002, **124**, 10942–10943.

69 T. Liu, E. Diemann, H. Li, A. W.-M. Dress and A. Müller, Self-assembly in aqueous solution of wheel-shaped Mo_{154} oxide clusters into vesicles, *Nature*, 2003, **426**, 59–62.

70 T. Liu, An unusually slow self-assembly of inorganic ions in dilute aqueous solution, *J. Am. Chem. Soc.*, 2003, **125**, 312–313.

71 G. Liu and T. Liu, Strong attraction among the fully hydrophilic $\{Mo_{72}Fe_{30}\}$ macroions, *J. Am. Chem. Soc.*, 2005, **127**, 6942–6943.

72 G. Liu, T. Liu, S. S. Mal and U. Kortz, Wheel-shaped polyoxotungstate $[Cu_{20}Cl(OH)_{24}(H_2O)_{12}(P_8W_{48}O_{184})]^{25-}$ macroanions from supramolecular ''Blackberry'' structure in aqueous solution, *J. Am. Chem. Soc.*, 2006, **128**, 10103–10110.

73 T. Liu, B. Imber, E. Diemann, G. Liu, K. Cokleski, H. Li, Z. Chen and A. Müller, Deprotonations and charges of well-defined $\{Mo_{72}Fe_{30}\}$ nanoacids simply stepwise tuned by pH allow control/variation of related self-assembly processes, *J. Am. Chem. Soc.*, 2006, **128**, 15914–15920.

74 A. A. Verhoeff, M. L. Kistler, A. Bhatt, J. Pigga, J. Groenwold, M. Klokkenburg, S. Veen, S. Roy, T. Liu and W. K. Kegel, Charge regulation as a stabilization mechanism for shell-like assemblies of polyoxometalates, *Phys. Rev. Lett.*, 2007, **99**, 066104.

75 C. Schäffer, A. Merca, H. Bögge, A. M. Todea, M. L. Kistler, T. Liu, R. Thouvenot, P. Gouzerh and A. Müller, Unprecedented and differently applicable pentagonal units in a dynamic library: A Keplerate of the type $\{(W)W_5\}_{12}\{Mo_2\}_{30}$, *Angew. Chem., Int. Ed.*, 2008, **48**, 149–153.

76 M. L. Kistler, T. Liu, P. Gouzerh, A. M. Todea and A. Müller, Molybdenum-oxide based unique polyprotic nanoacids showing different deprotonations and related assembly processes in solution, *Dalton Trans.*, 2009, 5094–5100.

77 P. Gouzerh and A. Proust, Main-group element, Organic, and Organometallic derivatives of polyoxometalates, *Chem. Rev.*, 1998, **98**, 77–112.

78 H. Kwen, V. G. Young and E. A. Maatta, A diazoalkane derivative of a polyoxometalate: Preparation and structure of $[Mo_6O_{18}(NNC(C_6H_4OCH_3)(CH_3)]^{2-}$, *Angew. Chem., Int. Ed.*, 1999, **38**, 1145–1146.

79 Z. Peng, Rational synthesis of covalently bonded organic-inorganic hybrids, *Angew. Chem., Int. Ed.*, 2004, **43**, 930–935.

80 Y. F. Song, D. L. Long and L. Cronin, Noncovalently connected frameworks with nanoscale channels assembled from a tethered polyoxometalate-pyrene hybrid, *Angew. Chem., Int. Ed.*, 2007, **46**, 3900–3904.

81 J. Hao, L. Ruhlmann, Y. Zhu, Q. Li and Y. Wu, Naphthylimido-substituted hexamolybdate: Preparation, crystal structures, solvent effects, and optical properties of three polymorphs, *Inorg. Chem.*, 2007, **46**, 4960–4967.

82 H. Liu, C. Qin, Y. G. Wei, L. Xu, G. G. Gao, F. Y. Li and X. S. Qu, Copper-complex-linked polytungsto-bismuthate (-antimonite) chain containing sandwich Cu(II) ions partially modified with imidazole ligand, *Inorg. Chem.*, 2008, **47**, 4166–4172.

83 C. P. Pradeep, M. F. Misdrahi, F. Y. Li, J. Zhang, L. Xu, D. L. Long, T. Liu and L. Cronin, Synthesis of modular ''Inorganic–Organic–Inorganic'' polyoxometalates and their assembly into vesicles, *Angew. Chem., Int. Ed.*, 2009, **48**, 8309–8313.

84 P. Yin, P. Wu, Z. Xiao, D. Li, E. Bitterlich, J. Zhang, P. Cheng, D. V. Vezenov, T. Liu and Y. Wei, A double-tailed fluorescent surfactant with a hexavanadate cluster as the head group, *Angew. Chem., Int. Ed.*, 2011, **50**, 2521–2525.

85 Y. Y. Bao, L. H. Bi, L. X. Wu, S. S. Mal and U. Kortz, Preparation and characterization of Langmuir–Blodgett films of wheel shaped Cu-20 tungstophosphate and DODA by two different strategies, *Langmuir*, 2009, **25**, 13000–13006.

86 H. Sun, H. Li and L. Wu, Micro-patterned polystyrene surfaces directed by surfactant-encapsulated polyoxometalate complex *via* breath figures, *Polymer*, 2009, **50**, 2113–2122.

87 P. Tang and J. Hao, Photoluminescent honeycomb films templated by microwater droplets, *Langmuir*, 2010, **26**, 3843–3847.

88 H. Sun, H. Li, W. Bu, M. Xu and L. Wu, Self-organized microporous structures based on surfactant-encapsulated

polyoxometalate complexes, *J. Phys. Chem. B*, 2006, **110**, 24847–24854.

89 Z. Kang, E. Wang, M. Jiang and S. Lian, Synthesis and characterization of polyoxometalate nanowires based on a novel microemulsion process, *Nanotechnology*, 2003, **15**, 55–58.

90 Y. Yan, B. Li, W. Li, H. Li and L. Wu, Controllable vesicular structure and reversal of a surfactant-encapsulated polyoxometalate complex, *Soft Matter*, 2009, **5**, 4047–4053.

91 C. Ritchie, G. J.-T. Cooper, Y. F. Song, C. Streb, H. Yin, A. D.-C. Parenty, D. A. MacLaren and L. Cronin, Spontaneous assembly and real-time growth of micro-metre-scale tubular structures from polyoxometalate-based inorganic solids, *Nat. Chem.*, 2009, **1**, 47–52.

92 G. J.-T. Cooper, A. G. Boulay, P. J. Kitson, C. Ritchie, C. J. Richmond, J. Thiel, D. Gabb, R. Eadie, D. L. Long and L. Cronin, Osmotically driven crystal morphogenesis: A general approach to the fabrication of micrometer-scale tubular architecture based on polyoxometalates, *J. Am. Chem. Soc.*, 2011, **133**, 5947–5954.

93 A. Nisar and X. Wang, Surfactant-encapsulated polyoxometalate building blocks: Controlled assembly and their catalytic properties, *Dalton Trans.*, 2012, **41**, 9832–9845.

94 D. G. Kurth, P. Lehmann, D. Volkmer, H. Cölfen, M. J. Koop, A. Müller and A. Du, Chesne, Surfactant-encapsulated clusters (SECs): $(DODA)_{20}(NH_4)[H_3Mo_{57}V_6(NO)_6O_{183}(H_2O)_{18}]$, a case study, *Chem. – Eur. J.*, 2000, **6**, 385–393.

95 W. Bu, H. Li, H. Sun, S. Yin and L. Wu, Polyoxometalate-based vesicle and its honeycomb architectures on solid surfaces, *J. Am. Chem. Soc.*, 2005, **127**, 8016–8017.

96 J. Zhang, Y. F. Song, L. Cronin and T. Liu, Self-assembly of organic-inorganic hybrid amphiphilic surfactants with large polyoxometalates as polar head groups, *J. Am. Chem. Soc.*, 2008, **130**, 14408–14409.

97 B. Zhang, P. Yin, F. Haso, L. Hu and T. Liu, Soft matter approaches for enhancing the catalytic capabilities of polyoxometalate clusters, *J. Cluster Sci.*, 2014, **25**, 695–710.

98 X. Yan, P. Zhu, J. Fei and J. Li, Self-assembly of peptide-inorganic hybrid spheres for adaptive encapsulation of guests, *Adv. Mater.*, 2010, **22**, 1283–1287.

99 C. Tan and R. Feng, Self-assembly morphology and packing structures depend on the ''head'' of organic cations anchored on polyoxometalate anions in hybrids, *Supramol. Chem.*, 2017, **29**, 634–642.

100 A. M. Todea, J. Szakács, S. Konar, H. Bögge, D. C. Crans, T. Glaser, T. Rousselière, R. Thouvenot, P. Gouzerh and A. Müller, Reduced molybdenum-oxide based core-shell hybrids: ''Blue'' electrons are delocalized on the shell, *Chem. – Eur. J.*, 2011, **17**, 6635–6642.

101 P. Zhao, Y. Leng and J. Wang, Heteropolyanion-paired cross-linked ionic copolymer: An efficient heterogeneous catalyst for hydroxylation of benzene with hydrogen peroxide, *Chem. Eng. J.*, 2012, **204-206**, 72–78.

102 R. X. Yao, X. Cui, X. X. Jia, F. Q. Zhang and X. M. Zhang, A luminescent Zn(II) metal–organic framework (MOF) with conjugated π-electron ligand for high iodine capture and nitro-explosive detection, *Inorg. Chem.*, 2016, **55**, 9270–9275.

103 A. Yamaguchi, R. B. Penland, S. Mizushima, T. J. Lane, C. Curran and J. V. Quagliano, Infrared absorption spectra of inorganic coordination complexes. XIV. Infrared studies of some metal thiourea complexes, *J. Am. Chem. Soc.*, 1958, **80**, 527–529.

104 X. Zhang, Z. Cui, Z. Cheng, Y. Li and H. Xiao, Quantitative detection of H_2S and CS_2 mixed gases based on UV absorption spectrometry, *RSC Adv.*, 2017, **7**, 50889–50898.